Intramolecular Energy Transfer in (diimine)$Re^{I}(CO)_3$–[CpM^{II}(arene)] Dimers

Yingsheng Wang and Kirk S. Schanze*

Department of Chemistry, University of Florida, Gainesville, Florida 32611

Received July 1, 1993®

This report presents the photochemistry and photophysics of the series of dimeric complexes *fac*-(b)$Re^{I}(CO)_3$–[CpM^{II}(arene)]$^{2+}$, where b = a series of substituted 2,2′-bipyridine ligands, Cp = η^5-cyclopentadienyl, and M = Fe and Ru. The two metals are linked by 4-benzylpyridine, which is coordinated η^1 to Re(I) via the pyridyl nitrogen and η^6 to M(II) via the benzyl group. Near-UV photoexcitation of these complexes produces the luminescent dπ (Re) → π^* (diimine) metal-to-ligand charge-transfer (MLCT) state. The MLCT state is quenched by intramolecular exchange energy transfer (E_NT) to the reactive ^{3}d–d state of CpM(arene). Evidence that E_NT occurs is provided by the observation of the following reaction during Re → diimine MLCT photoexcitation: (b)$Re^{I}(CO)_3$–[CpM^{II}(arene)]$^{2+}$ $\xrightarrow{h\nu,CH_3CN}$ (b)$Re^{I}(CO)_3$(4-benzylpyridine)$^+$ + $CpM(CH_3CN)_3^+$. The driving force for Re → M E_NT (ΔE_{E_NT}) is varied by changing the energy of the Re → diimine MLCT state and by varying M. For M = Ru, E_NT is weakly endothermic, and for M = Fe, E_NT is moderately exothermic. The rate of intramolecular E_NT is estimated from the quantum efficiency for CpM(arene) loss from the dimers and from MLCT emission lifetimes. The activation energy and frequency factor for E_NT in the (b)Re–Ru series is determined from the temperature dependence of the MLCT emission decay rate.

Introduction

The *fac*-(b)$Re^{I}(CO)_3$–L chromophore (where b is a diimine ligand such as 2,2′-bipyridine) has been used extensively in a number of recent studies of photoinduced intramolecular energy and electron transfer (E_NT and ET, respectively).[1-19] This system is particularly convenient for such studies because the energy and redox potentials of the dπ (Re) → π^* (diimine) metal-to-ligand charge-transfer (MLCT) excited state can be systematically tuned over a wide range by varying the substituents on the diimine acceptor ligand.[15,20] Studies with this system have revealed a variety of results concerning the free energy dependence of the rates of intramolecular E_NT and ET.

In a recent series of papers, Mann and co-workers outlined the unique synthetic and photochemical properties of a series of CpM^{II}(arene) complexes, where M = Ru or Fe, Cp = η^5-cyclopentadienyl, and arene is a wide range of mono- or polycyclic aromatic compounds that are ligated η^6 to M.[21-30] Two of the more significant findings of this work are (1) that a remarkably wide range of arenes can be easily incorporated into the synthesis of the complexes and (2) that population of the ^{3}d–d excited state of CpM(arene) leads to exceedingly fast and relatively efficient release of the free arene ligand.

Our interest in application of the (b)$Re^{I}(CO)_3$– chromophore to the study of intramolecular E_NT led us to consider the photophysical and photochemical consequences of covalently attaching the CpM(arene) unit to the Re chromophore. Previous photochemical and spectroscopic work on CpM(arene) complexes suggested that E_NT from the Re → diimine MLCT state to the ^{3}d–d state of CpM(arene) would be slightly endothermic for M = Ru and moderately exothermic for M = Fe.[29] Since photorelease of arene from CpM(arene) is exceedingly rapid, E_NT from Re MLCT to CpM(arene) d–d will be irreversible.[31,32] This fact suggested that development of a binuclear complex that incorporates both (b)$Re^{I}(CO)_3$– and CpRu(arene) chromophores would afford the unique opportunity to study endothermic *intramolecular* E_NT.

This paper presents a detailed report concerning the photophysics and photochemistry of the series of binuclear complexes (b)Re–M and the corresponding monomeric complexes (b)Re. (In this acronym, b refers to the following diimine ligands: bpy = 2,2′-bipyridine, dmb = 5,5′-dimethyl-2,2′-bipyridine, tmb = 4,4′,5,5′-tetramethyl-2,2′-bipyridine, deab = 4,4′-bis(diethylamino)-2,2′-bipyridine.) In this series the energy of the Re → diimine MLCT excited state is varied over a 2000-cm^{-1} range. Photoexcitation of the dimers in the near-UV region leads predominantly to formation of the Re MLCT state, and photophysical and photochemical results indicate that E_NT from Re to CpM(arene)

* Abstract published in *Advance ACS Abstracts*, February 15, 1994.

(1) Westmoreland, T. D.; Schanze, K. S.; Neveaux, P. E., Jr.; Danielson, E.; Sullivan, B. P.; Chen, P.; Meyer, T. J. *Inorg. Chem.* **1985**, *24*, 2596.
(2) Chen, P.; Westmoreland, T. D.; Danielson, E.; Schanze, K. S.; Anthon, D.; Neveaux, P. E., Jr.; Meyer, T. J. *Inorg. Chem.* **1987**, *26*, 1116.
(3) Chen, P.; Danielson, E.; Meyer, T. J. *J. Phys. Chem.* **1988**, *92*, 3708.
(4) Chen, P.; Duesing, R.; Tapolsky, G.; Meyer, T. J. *J. Am. Chem. Soc.* **1989**, *111*, 8305.
(5) Tapolsky, G.; Duesing, R.; Meyer, T. J. *J. Phys. Chem.* **1989**, *93*, 3885.
(6) Chen, P.; Curry, M.; Meyer, T. J. *Inorg. Chem.* **1989**, *28*, 2271.
(7) Duesing, R.; Tapolsky, G.; Meyer, T. J. *J. Am. Chem. Soc.* **1990**, *112*, 5378.
(8) Chen, P.; Duesing, R.; Graff, D. K.; Meyer, T. J. *J. Phys. Chem.* **1991**, *95*, 5850.
(9) Perkins, T. A.; Hauser, B. T.; Eyler, J. R.; Schanze, K. S. *J. Phys. Chem.* **1990**, *94*, 8745.
(10) Cabana, L. A.; Schanze, K. S. *Adv. Chem. Ser.* **1990**, *226*, 101.
(11) Schanze, K. S.; Cabana, L. A. *J. Phys. Chem.* **1990**, *94*, 2740.
(12) MacQueen, D. B.; Schanze, K. S. *J. Am. Chem. Soc.* **1991**, *113*, 7470.
(13) MacQueen, D. B.; Eyler, J. R.; Schanze, K. S. *J. Am. Chem. Soc.* **1992**, *114*, 1897.
(14) Thornton, N. B.; Schanze, K. S. *Inorg. Chem.* **1993**, *32*, 4994.
(15) Schanze, K. S.; MacQueen, D. B.; Perkins, T. A.; Cabana, L. A. *Coord. Chem. Rev.* **1993**, *122*, 63.
(16) Wang, Y.; Burton, R. D.; Hauser, B. T.; Rooney, M. M.; Schanze, K. S. *J. Am. Chem. Soc.* **1993**, *115*, 5675.
(17) Yoon, D. I.; Berg-Brennan, C. A.; Lu, H.; Hupp, J. T. *Inorg. Chem.* **1992**, *31*, 3192.
(18) Furue, M.; Naiki, M.; Kanematsu, Y.; Kushida, T.; Kamachi, M. *Coord. Chem. Rev.* **1991**, *111*, 221.
(19) Berg-Brennan, C. A.; Yoon, D. I.; Hupp, J. T. *J. Am. Chem. Soc.* **1993**, *115*, 2048.
(20) Worl, L. A.; Duesing, R.; Chen, P.; Della Ciana, L.; Meyer, T. J. *J. Chem. Soc., Dalton Trans.* **1991**, 849.
(21) Schrenk, J. L.; Palazzotto, M. C.; Mann, K. R. *Inorg. Chem.* **1983**, *22*, 4047.
(22) Gill, T. P.; Mann, K. R. *Inorg. Chem.* **1980**, *19*, 3007.
(23) Gill, T. P.; Mann, K. R. *Inorg. Chem.* **1983**, *22*, 1986.
(24) McNair, A. M.; Schrenk, J. L.; Mann, K. R. *Inorg. Chem.* **1984**, *23*, 2633.
(25) McNair, A. M.; Boyd, D. C.; Bohling, D. A.; Gill, T. P.; Mann, K. R. *Inorg. Chem.* **1987**, *26*, 1182.
(26) Koefod, R. S.; Mann, K. R. *Inorg. Chem.* **1989**, *28*, 2285.
(27) Freedman, D. A.; Mann, K. R. *Inorg. Chem.* **1989**, *28*, 3926.
(28) Koefod, R. S.; Mann, K. R. *J. Am. Chem. Soc.* **1990**, *112*, 7287.
(29) Koefod, R. S.; Mann, K. R. *Inorg. Chem.* **1991**, *30*, 541.
(30) Koefod, R. S.; Mann, K. R. *Inorg. Chem.* **1991**, *30*, 2221.
(31) Chrisope, D. R.; Park, K. M.; Schuster, G. B. *J. Am. Chem. Soc.* **1989**, *111*, 6195.
(32) Park, K. M.; Schuster, G. B. *J. Organomet. Chem.* **1991**, *402*, 355.

0020-1669/94/1333-1354$04.50/0

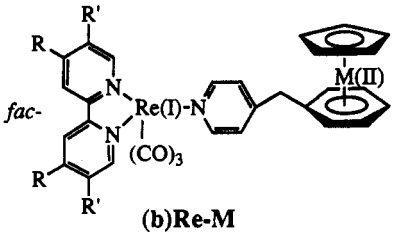

(b)Re-M

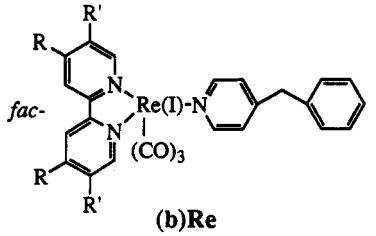

(b)Re

occurs with an efficiency that varies strongly with the energy of this state. Analysis of photochemical reaction efficiencies and the temperature dependence of MLCT emission lifetimes leads to estimates for the rate constants and activation parameters for intramolecular endothermic E_NT in the Re–Ru series.

Experimental Section

General Procedures. Solvents and chemicals used for synthesis were of reagent grade and were used without purification unless noted. 5,5′-Dimethyl-2,2′-bipyridine (dmb) and 4,4′,5,5′-tetramethyl-2,2′-bipyridine were synthesized according to a literature procedure.[33] All transition metal complexes were purified by repeated chromatography on either silica gel (Merck, 230–400 mesh) or neutral alumina (Fisher, Brockman Grade III). Proton and carbon NMR spectra were obtained on a GE QE-300 instrument.

4,4′-Bis(diethylamino)-2,2′-bipyridine (deab) was synthesized via a modification of the literature procedure as described below.[34,35]

(a) 2,2′-Bipyridine 1,1′-Dioxide (1). A mixture of 6.5 g (41.6 mmol) of 2,2′-bipyridine, 30 mL of acetic acid, and 30 mL of 30% aqueous hydrogen peroxide was placed in a three-necked round-bottom flask. The solution was stirred and heated to 51 °C for 40 h. The resulting bright yellow transparent solution was then evaporated carefully first under reduced pressure while the temperature was increased gradually to 60 °C until no more liquid distilled and then by vacuum roto-vap to dryness to yield a pale yellow crystalline solid. The solid was placed in a drying pistol overnight to yield 8.8 g of dry product (90%). Spectral data: ^{1}H NMR (300 MHz, D_2O) δ 7.71–7.75 (m, 2 H), 7.81 (d, J = 7.2 Hz, 1 H), 8.44 (d, J = 7.2 Hz, 1 H); ^{13}C NMR (75 MHz, D_2O) δ 128.5 (CH), 128.9 (CH), 131.5 (CH), 139.8 (CH), 141.8 (C); LRMS (CI/ISOBUT): M + 1, m/z 189.

(b) 4,4′-Dinitro-2,2′-bipyridine 1,1′-Dioxide (2). Dioxide **1** (1.55 g, 8.2 mmol) was dissolved in 3.5 mL of concentrated sulfuric acid, and this solution was added to a mixture of 5 mL of fuming nitric acid and 3 mL of concentrated sulfuric acid that was contained in a three-necked round-bottom flask. The mixture was heated to 90 °C for 2 h. It was then cooled to room temperature and poured into 150 g ice in an Erlenmeyer flask to give a light yellow transparent solution. An aqueous solution of sodium hydroxide (80 mL, 4 M) was added under cooling and vigorous stirring until the solution was only slightly acidic (pH ≈ 5–6). At this time, a copious amount of precipitate formed. After a period of stirring, the yellow solid was collected by filtration, washed with ethanol, and then dried in vacuo overnight to yield 420 mg (20%) of dried product. Spectral data: ^{1}H NMR (300 MHz, DMSO) δ 8.35 (dd, J_1 = 7.2 Hz, J_2 = 3.3 Hz, 1 H), 8.57 (d, J = 7.2 Hz, 1 H), 8.67 (d, J = 3.3 Hz, 1 H); ^{13}C NMR (75 MHz, DMSO) δ 122.3 (CH), 124.2 (CH), 140.9 (CH), 141.6 (C), 142.5 (C); LRMS (CI/ISOBUT) M + 1, m/z 279.

(c) 4,4′-Dichloro-2,2′-bipyridine 1,1′-Dioxide (3). A mixture of 420 mg (1.5 mmol) of **2**, 10 mL of acetic acid, and 20 mL of acetyl chloride was placed in a three-necked round-bottom flask and heated to ≈50 °C with stirring for 2 h. The solid dissolved in the solvent upon heating. Unreacted acetyl chloride was removed by evaporation, and the remaining yellow transparent solution (ca. 10 mL) was poured onto 100 g of ice. Aqueous sodium carbonate (12 mL, 15% Na_2CO_3) was then added with stirring. At this time, a yellow precipitate formed. The solid was collected by filtration, washed with methanol, and then placed in vacuo overnight to yield 210 mg (54%) of an off-white solid. Spectral data: ^{1}H NMR (300 MHz, CD_3CO_2D) δ 7.73 (dd, J_1 = 6.9 Hz, J_2 = 2.7 Hz, 1 H), 7.87 (d, J = 2.7 Hz, 1 H), 8.66 (d, J = 6.9 Hz, 1 H); ^{13}C NMR (75 MHz, CD_3COOD) δ 128.0 (CH), 128.8 (CH), 136.5 (C), 141.6 (CH), 142.1 (C).

(d) 4,4′-Bis(diethylamino)-2,2′-bipyridine 1,1′-Dioxide (4). A suspension of 170 mg (0.66 mmol) of **3**, 1.4 mL of diethylamine, and 1.0 mL of H_2O was heated in a sealed tube for 16 h at 130–140 °C. After cooling of the mixture to room temperature, diethylamine and H_2O were removed by vacuum roto-vap leaving a brown oily residue, which was then dissolved in small volume of CH_2Cl_2, and the solution was dropped into dry ether to yield a dark yellow solid, 133 mg (61%). Spectral data: ^{1}H NMR (300 MHz, CD_3CN) δ 1.21 (t, J = 6.9 Hz), 12 H), 3.56 (q, J = 6.9 Hz, 8 H), 6.95 (dd, J_1 = 7.8 Hz, J_2 = 3.3 Hz, 2 H), 7.05 (d, J = 3.3 Hz, 2 H), 8.15 (d, J = 7.8 Hz, 2 H).

(e) 4,4′-Bis(diethylamino)-2,2′-bipyridine (deab). A mixture of 133 mg (0.4 mmol) of **4** and 3 mL of dry $CHCl_3$ was placed in a three-necked round-bottom flask and cooled to 0 °C by using an ice bath. PCl_3 (1 mL) was added to the flask by syringe. The mixture was then heated to reflux for 1.5 h. The resulting solution was poured into 400 mL of ice water, and the $CHCl_3$ layer was separated from the mixture. The yellow aqueous layer was then placed in an Erlenmeyer flask, and 6 M aqueous sodium hydroxide solution was added with stirring. The solution turned from yellow to brown, and at pH ≈ 7, precipitate began to form. The NaOH solution was added until no more precipitate formed. The solid was collected by filtration, washed with H_2O, and then placed in vacuo to yield 60 mg of a gray black powder (50%). Spectral data: ^{1}H NMR (300 MHz, CD_3CN) δ 1.18 (t, J = 6.6 Hz, 12 H, methyl), 3.44 (q, J = 6.6 Hz, 8 H, methylene), 6.57 (d, J = 5.4 Hz, 2 H, bipyridyl), 7.68 (s, 2 H, bipyridyl), 8.16 (d, J = 5.4 Hz, 2 H, bipyridyl); ^{13}C NMR (75 MHz, CD_3CN) δ 11.4 (methyl), 43.3 (methylene), 102.7, 105.9, 148.8, 152.6, 156.4 (all aromatic).

[(η^5-C_5H_5)Ru(CH_3CN)$_3$]PF_6 was synthesized by literature procedures.[36–38] Spectral data: ^{1}H NMR (300 MHz, CD_3CN) δ 4.27 (s, η^5-Cp); ^{13}C NMR (75 MHz, CD_3CN): δ 68.4 (η^5-C_5H_5).

[(η^5-C_5H_5)Fe(η^6-4-benzylpyridine]PF_6.[39] A mixture of 6.6 g (35 mmol) of ferrocene, 10 g of $AlCl_3$ (anhydrous), 1 g of Al powder, and 40 mL of methylcyclohexane were placed in a 200-mL three-necked round-bottom flask equipped with a mechanical stirring motor, under a blanket of nitrogen. 4-Benzylpyridine (6 mL, 38 mmol) was then added to the flask, and the mixture was heated to reflux for 24 h. After cooling, the upper orange layer was removed from the flask by using a pipet, leaving behind a sticky residue in the flask. At this point, 50 g of ice and 20 mL of methylcyclohexane were added to the flask. The mixture was stirred until all of the residue dissolved, and the resulting solution was filtered. The greenish aqueous layer in the filtrate was then isolated and washed twice with methylcyclohexane. Addition of the aqueous solution to 20 mL of an aqueous solution containing 6 g of NH_4PF_6 with stirring produced a yellow-green precipitate, which was collected by filtration and washed with H_2O and then pentane. The solid was placed in vacuo to yield 6.0 g of product (40%). Spectral data: ^{1}H NMR (300 MHz, CD_3CN) δ 4.41 (s, 2 H, benzylic), 5.08 (s, 5 H, Cp), 6.29 (s, 5 H, C_6H_5), 7.86 (d, J = 6.0 Hz, 2 H, pyridyl), 8.61 (d, J = 6.0 Hz, 2 H, pyridyl); ^{13}C NMR (75 MHz, CD_3CN) δ 39.4 (benzylic), 77.2 (η^5-Cp), 87.4, 87.9, 88.6, 101.6 (η^6-C_6H_5), 127.2, 141.3, 159.9 (pyridyl).

(b)Re Monomers. These complexes were synthesized by previously described procedures.[12] Typical yields after chromatography were 50–60%. ^{1}H NMR (300 MHz) and ^{13}C NMR (75 MHz) were run in CD_3CN for all (b)Re monomer complexes.

(bpy)Re. Spectral data: ^{1}H NMR δ 3.92 (s, 2 H, benzylic), 7.11 (d, J = 6.6 Hz, 2 H, pyridyl), 7.1–7.3 (m, 5 H, phenyls), 7.76 (d of d, J_1 = 7.5 Hz, J_2 = 5.4 Hz, 2 H, bipyridyl), 8.09 (d, J = 6.6 Hz, 2 H, pyridyl), 8.25 (d of d, J_1 = 8.1 Hz, J_2 = 7.5 Hz, 2 H, bipyridyl), 8.37 (d, J = 8.1 Hz, 2 H, bipyridyl), 9.19 (d, J = 5.4 Hz, 2 H, bipyridyl); ^{13}C NMR δ

(33) Cook, M. J.; Lewis, A. P.; McAuliffe, G. S. G.; Skarda, V.; Thomsen, A. J.; Glaspar, J. L.; Robbins, D. J. *J. Chem. Soc., Perkin Trans. 2* **1984**, 1293.
(34) Den Herdog, H. J.; Combe, W. P. *Recl. Trav. Chim. Pays-Bas* **1951**, *70*, 581.
(35) Maerker, G.; Case, F. H. *J. Am. Chem. Soc.* **1958**, *80*, 2745.
(36) Zelonka, R. A.; Baird, M. C. *Can. J. Chem.* **1972**, *50*, 3063.
(37) Zelonka, R. A.; Baird, M. C. *J. Organomet. Chem.* **1972**, *44*, 383.
(38) Gill, T. P.; Mann, K. R. *Organometallics* **1982**, *1*, 485.
(39) Sutherland, R. G.; Chen, S. C.; Pannekoek, J.; Lee, C. C. *J. Organomet. Chem.* **1975**, *101*, 221.

39.9 (benzylic), 124.4, 126.4, 126.6, 128.5, 128.5, 128.7, 137.7, 140.8, 151.3, 153.5, 155.0, 155.5 (all aromatic).

(dmb)Re. Spectral data: ^{1}H NMR δ 2.52 (s, 6 H, methyl), 3.93 (s, 2 H, benzylic), 7.1–7.3 (m, 7 H, pyridyl and phenyls), 8.03 (d, J = 8.4 Hz, 2 H, bipyridyl), 8.14 (d, J = 6.6 Hz, 2 H, pyridyl), 8.17 (d, J = 8.4 Hz, 2 H, bipyridyl), 8.99 (s, 2 H, bipyridyl); ^{13}C NMR δ 17.2 (methyl), 39.9 (benzylic), 123.3, 126.3, 126.6, 128.5, 128.8, 137.8, 139.4, 141.0, 151.5, 153.0, 153.3, 155.0 (all aromatic).

(tmb)Re. Spectral data: ^{1}H NMR δ 2.41 (s, 6 H, methyl), 2.44 (s, 6 H, methyl), 3.93 (s, 2 H, benzylic), 7.10 (d, J = 6.6 Hz, 2 H, pyridyl), 7.1–7.4 (m, 5 H, phenyls), 8.10 (s, 2 H, bipyridyl), 8.13 (d, J = 6.6 Hz, 2 H, pyridyl), 8.84 (s, 2 H, bipyridyl); ^{13}C NMR δ 15.5 (methyl), 18.7 (methyl), 39.9 (benzylic), 124.2, 126.2, 126.6, 128.6, 128.7, 137.8, 138.3, 151.5, 152.2, 152.3, 153.2, 154.9 (all aromatic).

(deab)Re. Spectral data: ^{1}H NMR δ 1.19 (t, J = 6.9 Hz, 12 H, methyl), 3.54 (q, J = 6.9 Hz, 8 H, methylene), 3.95 (s, 2 H, benzylic), 6.75 (d, J = 6.9 Hz, 2 H, bipyridine), 7.17 (s, 2 H, bipyridyl), 7.1–7.3 (m, 7 H, pyridyl and phenyls), 8.14 (d, J = 6.3 Hz, 2 H, pyridyl), 8.45 (d, J = 6.9 Hz, 2 H, bipyridyl); ^{13}C NMR δ 11.0 (methyl), 39.9 (benzylic), 44.0 (methylene), 104.7, 109.9, 126.1, 126.6, 128.6, 128.7, 137.9, 151.3, 151.7, 153.3, 154.6, 155.9 (all aromatic).

General Procedure for Preparation of (b)Re–Ru Dimers.[40] These complexes were prepared and purified under dim lights to minimize exposure of the complexes to light. In a typical preparation, 60 mg of $[(\eta^5\text{-}C_5H_5)Ru(CH_3CN)_3]PF_6$ (0.14 mmol) was added under positive nitrogen pressure to a 1,2-dichloroethane solution of 101 mg (0.13 mmol) of (tmb)Re. The solution was degassed with nitrogen for an additional 20 min and then heated to reflux for 14 h. The resulting solution was evaporated to dryness, and the crude product was purified by chromatography on alumina with 30% CH_3CN/CH_2Cl_2 as eluent. The combined fractions that contained the product were dissolved in CH_2Cl_2 and reprecipitated from ethyl ether to give the product as a pale yellow powder, yield 90 mg (65%). ^{1}H NMR (300 MHz) and ^{13}C NMR (75 MHz) were run in CD_3CN for all (b)Re–Ru dimers.

(bpy)Re–Ru. Spectral data: ^{1}H NMR δ 3.78 (s, 2 H, benzylic), 5.21 (s, 5 H, η^5-Cp), 6.03 (s, 5 H, η^6-C_6H_5), 7.19 (d, J = 6.3 Hz, 2 H, pyridyl), 7.79 (d of d, J_1 = 7.5 Hz, J_2 = 5.4 Hz, 2 H, bipyridyl), 8.18 (d, J = 6.3 Hz, 2 H, pyridyl), 8.26 (d of d, J_1 = 8.1 Hz, J_2 = 7.5 Hz, 2 H, bipyridyl), 8.37 (d, J = 8.1 Hz, 2 H, bipyridyl), 9.21 (d, J = 5.4 Hz, 2 H, bipyridyl); ^{13}C NMR δ 37.9 (benzylic), 80.6 (η^5-Cp), 84.9, 85.3, 86.6, 102.2 (η^6-C_6H_5), 124.4, 126.5, 128.6, 140.9, 151.5, 151.8, 153.6, 155.5 (all other aromatics).

(dmb)Re–Ru. Spectral data: ^{1}H NMR δ 2.53 (s, 6 H, methyl), 3.79 (s, 2 H, benzylic), 5.19 (s, 5 H, η^5-Cp), 6.03 (s, 5 H, η^6-C_6H_5), 7.19 (d, J = 6.0 Hz, 2 H, pyridyl), 8.03 (d, J = 8.4 Hz, 2 H, bipyridyl), 8.17 (d, J = 8.4 Hz, 2 H, bipyridyl), 8.23 (d, J = 6.0 Hz, 2 H, pyridyl), 9.00 (s, 2 H, bipyridyl); ^{13}C NMR δ 17.2 (methyl), 37.8 (benzylic), 80.6 (η^5-Cp), 84.9, 85.3, 86.6, 102.4 (η^6-C_6H_5), 123.4, 126.3, 139.5, 141.1, 151.5, 152.0, 153.0, 153.3 (all other aromatics).

(tmb)Re–Ru. Spectral data: ^{1}H NMR δ 2.42–2.43 (two peaks, not well resolved, 12 H, methyl), 3.79 (s, 2 H, benzylic), 5.15 (s, 5 H, η^5-Cp), 6.05 (s, 5 H, η^6-C_6H_5), 7.19 (d, J = 6.3 Hz, 2 H, pyridyl), 8.09 (s, 2 H, bipyridyl), 8.23 (d, J = 6.3 Hz, 2 H, pyridyl), 8.86 (s, 2 H, bipyridyl); ^{13}C NMR δ 15.5 (methyl), 18.7 (methyl), 37.7 (benzylic), 80.5 (η^5-Cp), 84.8, 85.3, 86.7, 102.7 (η^6-C_6H_5), 124.3, 126.3, 138.4, 151.6, 152.0, 152.3, 152.4, 153.2 (all other aromatics).

(deab)Re–Ru. Spectral data: ^{1}H NMR δ 1.18 (t, J = 6.9 Hz, 12 H, methyl), 3.52 (q, J = 6.9 Hz, 8 H, methylene), 3.80 (s, 2 H, benzylic), 5.10 (s, 5 H, η^5-Cp), 6.05 (s, broad, 5 H, η^6-C_6H_5), 6.76 (d, J = 6.6 Hz, 2 H, bipyridyl), 7.13 (s, 2 H, bipyridyl), 7.25 (d, J = 6.0 Hz, 2 H, pyridyl), 8.26 (d, J = 6.0 Hz, 2 H, pyridyl), 8.48 (d, J = 6.6 Hz, 2 H, bipyridyl); ^{13}C NMR δ 11.1 (methyl), 37.7 (benzylic), 44.0 (methylene), 80.5 (η^5-Cp), 84.8, 85.2, 86.7, 103.0 (η^6-C_6H_5), 104.7, 109.0, 126.2, 151.4, 151.8, 151.8, 153.3, 155.9 (all other aromatics).

(bpy)Re–Fe. The synthesis of this complex was carried out with minimum light exposure. A mixture of 250 mg (0.54 mmol) of (bpy)-$Re(CO)_3Cl$, 940 mg (2.16 mmol) of $[(\eta^5\text{-}C_5H_5)Fe(\eta^6\text{-}4\text{-benzylpyridine})]$-$PF_6$, 270 mg (1.08 mmol) of $AgPF_6$, and 20 mL of DMF was placed in a three-necked round-bottom flask under a blanket of nitrogen. The solution was heated to 75 °C for 24 h. During the course of the reaction, additional 100-mg protions of $AgPF_6$ were added on two separate occasions. The reaction was monitored by TLC until the high R_f spot for $(bpy)Re(CO)_3Cl$ had diminished entirely. At this point, the DMF was evaporated in vacuo and the residue was dissolved in CH_2Cl_2 and purified by chromatography on silica with gradient elution using mixtures ranging from pure CH_2Cl_2 to 30% CH_3CN/CH_2Cl_2. The combined fractions that contained the product were dissolved in CH_2Cl_2 and reprecipitated from *n*-pentane to give the product as a yellow powder, yield 160 mg (30%). Spectral data: ^{1}H NMR (300 MHz, $(CD_3)_2CO$) δ 4.29 (s, 2 H, benzylic), 5.17 (s, 5 H, η^5-Cp), 6.42 (s, 5 H, η^6-C_6H_5), 7.38 (d, J = 6.0 Hz, 2 H, pyridyl), 7.95 (d of d, J_1 = 7.5 Hz, J_2 = 5.4 Hz, 2 H, bipyridyl), 8.39–8.46 (m, 4 H, bipyridyl and pyridyl), 8.66 (d, J = 8.1 Hz, 2 H, bipyridyl), 9.40 (d, J = 5.4 Hz, 2 H, bipyridyl); ^{13}C NMR (75 MHz, $(CD_3)_2CO$) δ 38.9 (benzylic), 77.3 (η^5-Cp), 87.5, 88.2, 88.8, 103.3 (η^6-C_6H_5), 124.8, 126.7, 129.1, 141.4, 152.2, 152.3, 153.9, 155.8 (all other aromatics).

Photochemistry and Photophysics. Corrected steady-state emission spectra were recorded on a SPEX F-112 fluorimeter. Samples were contained in a 1 cm × 1 cm cell, and the optical density was adjusted to approximately 0.1 at the excitation wavelength. Emission quantum yields are reported relative to $Ru(bpy)_3^{2+}$ in H_2O (Φ_{em} = 0.055);[41] appropriate correction was applied for the difference in refractive indices of the sample and actinometer solvents.[42] Emission lifetimes were determined by time-correlated single-photon counting (FLI, Photochemical Research Associates). The excitation and emission wavelengths were selected by band-pass filters (excitation, Schott UG-11; emission, 550- or 600-nm interference filter). Lifetimes were calculated by using the DECAN deconvolution software on a 286 PC compatible computer.[43] Low-temperature lifetimes were obtained by cooling the samples in an Oxford Instruments DN-1704 optical cryostat. The acetonitrile and butyronitrile solvents used in the temperature-dependence studies were distilled prior to use.

Quantitative steady-state photochemical experiments were carried out using a 75-W high-pressure Hg arc lamp that is housed in an elliptical reflector housing (Photon Technology International, ALH-1000). The photolysis beam was passed through a monochromator and focused onto a 1 cm × 1 cm cell that contained a 3.0-mL aliquot of the sample. Actinometry was effected by using the Aberchrome 540 actinometer.[44] Samples were exposed to light for incremental periods of time, and then the concentration of reactant (or product) was determined by HPLC analysis. HPLC was carried out on a system composed of a Waters M-45 pump, a DuPont Zorbax ODS analytical column, and a Spectroflow 757 absorbance detector. The eluting solvent composition was THF/CH_3CN/H_2O (40:40:20 v/v/v) with 5 mM sodium heptanesulfonate.

Emission Spectral Fitting. A single-mode Franck–Condon line-shape analysis was used for emission spectral fitting.[20,42] The spectra were calculated using Microsoft BASIC 7.0 on a PC compatible computer, and the parameters were optimized by comparison of calculated and experimental spectra using a separate graphics package. The equation used to calculate the spectra is

$$I(\bar{\nu}) = \sum_{\nu_m=0}^{5}\left\{\left(\frac{\bar{\nu}_{00} - \nu_m\hbar\omega_m}{\bar{\nu}_{00}}\right)^3 \frac{S_m^{\nu_m}}{\nu_m!} \times \exp\left[-4\ln 2\left(\frac{\bar{\nu} - \bar{\nu}_{00} + \nu_m\hbar\omega_m}{\Delta\bar{\nu}_{0,1/2}}\right)^2\right]\right\} \quad (1)$$

where $I(\bar{\nu})$ is the relative emission intensity at frequency $\bar{\nu}$, $\bar{\nu}_{00}$ is the 0–0 emission energy, $\hbar\omega_m$ is the average of medium frequency acceptor modes that are coupled to the MLCT transition, S_m is the electron–vibration coupling constant (Huang–Rhys factor), $\Delta\bar{\nu}_{0,1/2}$ is the half-width of the 0–0 vibronic band, and the sum is taken over ν_m, the quantum number of the average medium frequency vibrational mode. A value of $\hbar\omega_m$ = 1450 cm^{-1} was used in all of the fits.[20]

Results

A. Photophysics of (b)Re Monomers. Figure 1 illustrates the UV–visible absorption spectra of (bpy)Re–Ru and the corresponding monomer, (bpy)Re. This figure highlights the fact that the entire absorption spectrum is dominated by transitions localized on the Re chromophore; CpRu(arene) contributes less than 10% to the total absorption of the dimer for λ < 370 nm. The shoulder in the near-UV ($\lambda \approx$ 340–410 nm) is assigned to

(40) McNair, A. M.; Mann, K. R. *Inorg. Chem.* **1986**, *25*, 2519.

(41) Harriman, A. *J. Chem. Soc., Chem. Commun.* **1977**, 777.

(42) Caspar, J. V. Ph.D. Thesis, The University of North Carolina at Chapel Hill, 1982.

(43) Boens, N.; De Roeck, T.; Dockx, J.; De Schryver, F. C. *DECAN* (v 1.0); 1991.

(44) Heller, H. G.; Langan, J. R. *J. Chem. Soc., Perkin Trans. 1* **1981**, 341.

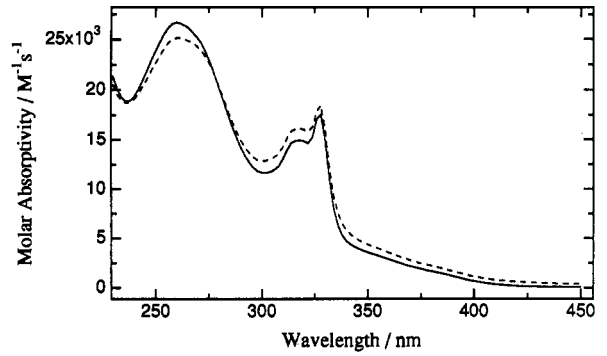

Figure 1. UV–visible absorption spectra in CH_3CN solution: (—) (bpy)-Re; (- - -) (bpy)Re–Ru.

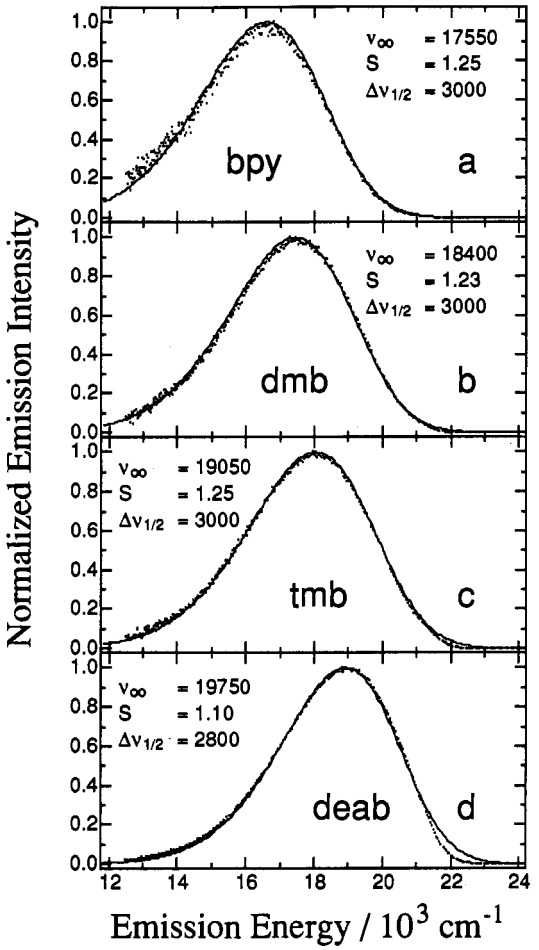

Figure 2. Corrected emission spectra of (b)Re monomer complexes in CH_3CN solution at 298 K: (a) (bpy)Re; (b) (dmb)Re; (c) (tmb)Re; (d) (deab)Re. Points are experimental data, and solid lines are spectra calculated using Franck–Condon analysis (see text). Parameters used for calculated spectra are printed on spectra.

the dπ (Re) → π^* (bpy) MLCT transition while the bands at higher energy are due to π,π^* intraligand (IL) and higher energy MLCT transitions based at (bpy)Re^{I}(CO)$_3$–. The spectra of the other (b)Re–M complexes are very similar to those illustrated in Figure 1.

All of the (b)Re monomers exhibit moderately intense emission that is attributed to the Re → diimine MLCT state. Figure 2 illustrates the spectra for the entire series, and the emission maxima ($\bar{\nu}_{max}$) and estimated 0–0 emission energies ($\bar{\nu}_{00}$; see below) are listed in Table 1. In every (b)Re complex the MLCT emissions appear as a broad, structureless envelopes with similar bandwidths. Note that the emission shifts to higher energy along the series bpy < dmb < tmb < deab. This shift in energy is consistent with the expected effect of the substituents on the LUMO energy of the diimine acceptor ligand.[15,20]

Table 1. Photophysical and Photochemical Properties of Monomeric and Dimeric Complexes[a]

ligand	metal	$\bar{\nu}_{max}$/cm^{-1} [c]	$\bar{\nu}_{00}$/cm^{-1} [d]	Φ_{em} [b]			τ_{em}/ns [b]			Φ_p [e]
				M	D	D/M	M	D	D/M	
bpy	Ru	17 060	17 550	0.045	0.051	1.1	208	225	1.1	0.002
dmb	Ru	17 820	18 400	0.18	0.16	0.89	950	960	1.0	0.03
tmb	Ru	18 520	19 050	0.26	0.15	0.58	1500	907	0.60	0.12
deab	Ru	19 120	19 750	0.31	0.041	0.12	9200	890	0.10	0.21
bpy	Fe	17 060	17 550	0.045	*f*	*f*	208	2.9	0.014	0.75

[a] Argon-degassed CH_3CN solution, 298 K. Estimated errors: $\bar{\nu}_{max}$, ±100 cm^{-1}; $\bar{\nu}_{00}$, ±500 cm^{-1}; Φ_{em}, ±15%; τ_{em}, ±5%; Φ_p, ±15%. [b] M = (b)Re monomer, D = (b)Re–M dimer, D/M = dimer/monomer ratio. [c] Emission maximum. [d] 0–0 emission energy; estimated by Franck–Condon analysis; see text. [e] Quantum yield for CpM(arene) loss from (b)Re–M dimer. [f] Compound is too photoreactive for determination.

Table 2. Radiative and Nonradiative Decay Rates for (b)Re Monomers and (b)Re–Ru Dimers[a]

ligand	$\bar{\nu}_{max}$/cm^{-1}	$k_r/10^5$ s^{-1} [b]			$k_{nr}/10^5$ s^{-1} [b]		
		M	D	D/M	M	D	D/M
bpy	17 060	2.2	2.3	1.0	46	42	0.91
dmb	17 820	1.9	1.9	1.0	8.6	8.5	0.99
tmb	18 520	1.7	1.6	0.94	4.9	9.4	1.9
deab	19 120	0.34	0.46	1.3	0.75	11	15

[a] Argon-degassed CH_3CN solutions, 298 K. Estimated error in rate constants is ±15%. [b] M = (b)Re monomer, D = (b)Re–M dimer, D/M = dimer/monomer ratio.

Owing to the fact that the MLCT emission is structureless, it is not possible to easily determine $\bar{\nu}_{00}$. Thus, in an effort to provide an estimate of this energy, the emission spectra were fitted by using a Franck–Condon line-shape analysis that has been successfully applied to analysis of MLCT emission of a wide range of related (diimine)M complexes.[20,42] The results of these spectral fits are provided in Figure 2; note that similar parameters were used to fit each spectrum, except for $\bar{\nu}_{00}$ (Table 1), which systematically increases along the aforementioned series. In general, the estimated $\bar{\nu}_{00}$ values are 500–600 cm^{-1} higher than ν_{max}.

Quantum yields and lifetimes for the MLCT emission (Φ_{em} and τ_{em}, respectively) in the (b)Re monomers at room temperature are listed in Table 1. Radiative and nonradiative decay rates (k_r and k_{nr}, respectively) for the MLCT state calculated from the emission parameters by using eqs 2 and 3 are listed in Table 2.

$$k_r = \Phi_{em}/\tau_{em} \quad (2)$$

$$k_{nr} = (1/\tau_{em}) - k_r \quad (3)$$

Note that Φ_{em} and τ_{em} increase in parallel as $\bar{\nu}_{max}$ increases. This trend is typical for structurally related series of MLCT chromophores and is due to a decrease in k_{nr} as the energy of the MLCT state increases (e.g., the energy gap law).[42,45–47] Consistent with this expectation, the data listed in Table 2 indicate that for the (b)Re monomers k_r is nearly constant and k_{nr} decreases along the series bpy > dmb > tmb > deab.

Inspection of all of the MLCT emission data reveals that (deab)-Re displays slightly anomalous emission parameters compared to the other complexes. In particular, the spectral fit requires a slightly lower $\Delta\nu_{0,1/2}$ and S_m value and the k_r value is unusually low for this complex. These subtle changes could signal that the lowest excited state for this complex has substantial configuration mixing between dπ (Re) → π^* (deab) MLCT and $^3\pi,\pi^*$ IL (deab) manifolds. This mixing may be important for (deab)Re due to the relatively high energy of the MLCT state.

(45) Caspar, J. V.; Kober, E. M.; Sullivan, B. P.; Meyer, T. J. *J. Am. Chem. Soc.* **1982**, *104*, 630.
(46) Caspar, J. V.; Sullivan, B. P.; Kober, E. M.; Meyer, T. J. *Chem. Phys. Lett.* **1982**, *91*, 91.
(47) Caspar, J. V.; Meyer, T. J. *Inorg. Chem.* **1983**, *22*, 2444.

B. Photophysics of (b)Re–M Dimers. As noted above, Figure 1 illustrates the absorption spectra of (bpy)Re and (bpy)Re–Ru for comparison. The important fact for the ensuing discussion is that, owing to the relatively weak UV (and visible) absorption of CpM(arene) (M = Ru and Fe), photoexcitation of all of the (b)Re–M dimers with $\lambda < 370$ nm excites almost exclusively transitions based at $(b)Re^{I}(CO)_3-$.

Near-UV photoexcitation (350 nm) of each (b)Re–Ru dimer produces MLCT emission that is identical in wavelength and band shape to the emission of the corresponding (b)Re monomers. Quantum yields and lifetimes for the MLCT emission are collected in Table 1, and radiative and nonradiative MLCT decay rate constants, calculated by using the emission parameters and eqs 2 and 3, are collected in Table 2. Although the band shape and energy of the MLCT emission are identical for each (b)Re–Ru dimer and (b)Re monomer pair, Φ_{em} and τ_{em} differ. First, for the complexes with the greatest $\bar{\nu}_{00}$ (b = deab and tmb), Φ_{em} and τ_{em} are depressed for the dimers compared to the monomers. By contrast, for the other two complexes with relatively lower $\bar{\nu}_{00}$ (b = dmb and bpy), Φ_{em} and τ_{em} are the same or slightly *greater* for the dimers compared to the corresponding monomers. Examination of the k_r and k_{nr} values for the complexes (Table 2) makes it possible to discern the origin of the variations observed in Φ_{em} and τ_{em} across the series. First, the k_r values for corresponding (b)Re monomer and (b)Re–Ru dimer pairs are the same within experimental error. By contrast, comparison of k_{nr} values reveals substantial deviations in several cases. Interestingly, the ratio k_{nr}(dimer)/k_{nr}(monomer) increases monotonically as $\bar{\nu}_{00}$ increases. This trend indicates that the rate of a nonradiative decay channel that operates in parallel with "normal" nonradiative decay of MLCT increases as $\bar{\nu}_{00}$ increases. This additional nonradiative process is very likely E_NT from Re → diimine MLCT to the CpRu(arene) d–d state.

In contrast to the situation for the (b)Re–Ru dimers, little or no MLCT emission is observed from (bpy)Re–Fe by using steady-state photon-counting spectroscopy. A weak, exceedingly short-lived emission (τ_{em} = 2.9 ns) is observed from the dimer by using time-correlated single-photon counting. These observations suggest that the Re → bpy MLCT state is quenched rapidly by E_NT to the CpFe(arene) d–d state.

C. Photochemistry of (b)Re–M Dimers. Irradiation of all of the (b)Re–Ru dimers (λ = 366 nm) leads to loss of CpRu(arene):

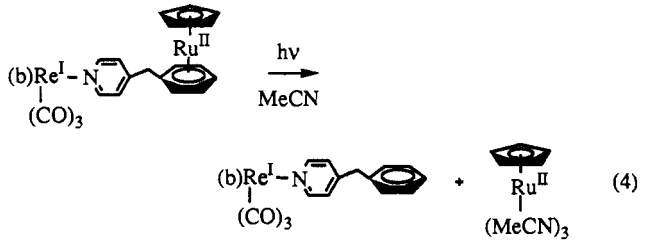

(4)

This reaction was studied by using NMR, which confirmed the stoichiometry expected based on eq 4. The quantum efficiency of the reaction (Φ_p) was determined for the series by using HPLC to monitor appearance of (b)Re (Table 1). While Φ_p is comparatively low for (bpy)Re–Ru, it increases substantially along the series bpy < dmb < tmb < deab. Note that Φ_p increases in parallel with the ratio k_{nr}(dimer)/k_{nr}(monomer) (Table 2); this fact strongly implies that Φ_p depends on the efficiency of Re → Ru E_NT.

Irradiation of (bpy)Re–Fe leads to highly efficient loss of CpFe(arene) from the dimer. Since the expected product of this reaction, $CpFe(CH_3CN)_3$, is thermally unstable,[22] eq 4 does not strictly apply to this system. However, NMR analysis indicates that disappearance of (bpy)Re–Fe and appearance of (bpy)Re occur with 1:1 stoichiometry; Φ_p for this reaction, determined by monitoring the appearance of (bpy)Re by HPLC, is given in Table 1.

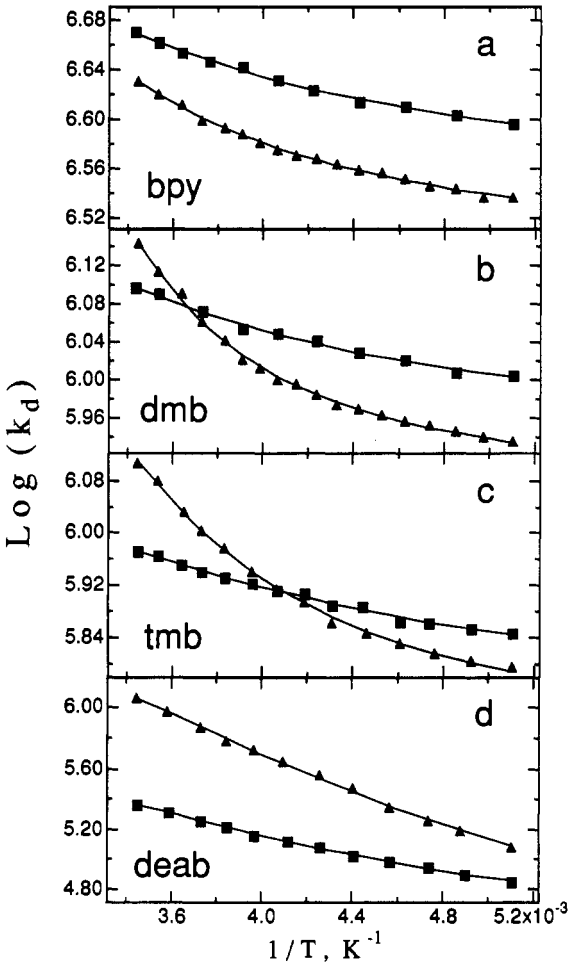

Figure 3. Temperature dependence of MLCT emission decay rate (k_d) in butyronitrile/acetonitrile (70:30 v/v) solution: (■) (b)Re monomers; (▲) (b)Re–Ru dimers; (a) b = bpy; (b) b = dmb; (c) b = tmb; (d) b = deab. Solid lines were calculated as described in the text.

D. Temperature Dependence of MLCT Emission for (b)Re Monomers and (b)Re–Ru Dimers. The temperature dependence of τ_{em} for MLCT emission of these complexes was examined over the temperature range 195–290 K in butyronitrile/acetonitrile (70:30 v/v). Figure 3 displays plots of the emission data as log k_d vs $1/T$, where $k_d = 1/\tau_{em}$. The emission decay rate of each (b)Re monomer decreases modestly as the temperature is decreased. By contrast, k_d is significantly more temperature dependent in the (b)Re–Ru dimers compared to the corresponding monomers. Another interesting point is that, for b = bpy, k_d(dimer) < k_d(monomer) at all temperatures; for b = dmb and tmb, k_d(dimer) > k_d(monomer) at high T, while k_d(dimer) < k_d(monomer) at low T; and for b = deab, k_d(dimer) > k_d(monomer) at all temperatures. Detailed analysis and discussion of the origin of the temperature-dependent emission properties of these complexes are provided below.

Discussion

A. Mechanism and Thermodynamics of Energy Transfer in (b)Re–M Dimers. The available photophysical data indicate that CpM(arene) perturbs the photophysics of the MLCT state in the (b)Re–M dimers. The magnitude of the perturbation depends strongly on the energy of the Re → diimine MLCT state and on whether M = Ru or Fe. Although CpM(arene) has some influence on the nonradiative decay rate of the localized MLCT state (k_{nr}), the predominant effect of CpM(arene) on the photophysics of the dimers is to allow MLCT decay via E_NT from MLCT to a d–d state of CpM(arene):

$$(b^{\bullet-})Re^{II}(CO)_3\text{–}[CpM(arene)] \xrightarrow{k_{E_NT}} Re \rightarrow diimine\ ^3MLCT \quad \Delta E_{E_NT}$$

$$(b)Re^{I}(CO)_3\text{–}^{*}[CpM(arene)] \quad (5)$$
$$^3d\text{–}d\ M$$

As indicated by this equation, E_NT very likely involves an MLCT state at Re and a d–d state at CpM(arene) that each have predominantly triplet spin character.[48-50] That E_NT occurs in all of (b)Re–Ru dimers is substantiated by the observation of photochemistry that must originate in a d–d state at CpM(arene) as a consequence of photoexcitation at wavelengths where most, if not all, of the incident light is absorbed by the (b)Re^{I}(CO)$_3$– chromophore.

Two mechanisms, Förster Coulombic and Dexter exchange, must be considered for this excited-state E_NT process.[51,52] The probability of E_NT via the Förster mechanism depends on the absolute value of the overlap integral between the emission and absorption spectra of the energy donor and acceptor, respectively. In order to achieve good overlap, appropriate energy matching is required and the transition probabilities for the emission and absorption processes of the donor and acceptor chromophores must be relatively large. Because of this latter consideration, the Förster mechanism is probable only for E_NT involving spin-allowed excited states at the two chromophores.[52] The Dexter exchange mechanism allows for electronic E_NT involving chromophores with spin-forbidden excited states. However, an important limitation of exchange E_NT is that it requires the donor and acceptor chromophores to be in close proximity because orbital overlap is required.[51] Because Re → M E_NT (eq 5) involves excited states having predominantly triplet spin character, it is very likely that the process occurs via Dexter exchange. The separation distance between the Re and Ru chromophores is sufficiently short that electronic coupling should be large enough to allow E_NT via the exchange mechanism.

The rate for exchange E_NT has been described by using theories that are similar to those used for nonadiabatic outer-sphere electron-transfer reactions.[53-56] In the semiclassical approximation, the rate for exchange E_NT is given by a Marcus expression

$$k_{E_NT} = k^{\circ}_{E_NT} \exp\left[-\frac{(\Delta E_{EN_T} - \lambda)^2}{4\lambda kT}\right] \quad (6)$$

where ΔE_{E_NT} is the energy gap between the localized excited states at the donor and acceptor, λ is the reorganization energy for E_NT, and $k^{\circ}_{E_NT}$ is the "maximum" E_NT rate, which is proportional to the square of the interchromophore electronic coupling matrix element (V_{el}^2). The important point for the present discussion is that eq 6 predicts that for endothermic and moderately exothermic E_NT (e.g., where $|\Delta E_{E_NT}| < \lambda$) k_{E_NT} increases as ΔE_{E_NT} becomes more exothermic (or less endothermic).

Since k_{E_NT} depends on ΔE_{E_NT}, it is important to provide an estimate for the latter quantity for the (b)Re–M dimers. The energy gap is calculated from the difference in the energies of the relevant excited states at the donor and acceptor chromophores:[54]

$$\Delta E_{E_NT} = \bar{\nu}_{00}^{\text{acceptor}} - \bar{\nu}_{00}^{\text{donor}} \quad (7)$$

In the (b)Re–M dimers $\bar{\nu}_{00}^{donor}$ and $\bar{\nu}_{00}^{acceptor}$ refer to the 0–0 energies of the Re → diimine MLCT and CpM(arene) d–d states, respectively. In order to estimate ΔE_{E_NT}, it is necessary to have estimates of $\bar{\nu}_{00}$ for ^{3}MLCT of (diimine)Re^{I}(CO)$_3$– and for ^{3}d–d of CpM(arene). For the (diimine)Re(CO)$_3$– chromophore, $\bar{\nu}_{00}$ values were estimated from fits of the MLCT emission (Table 1).

Considerable spectroscopic and Stern–Volmer quenching information is available concerning the energy of the ^{3}d–d state in the metallocenes, Cp_2M, which are structurally related to the CpM(arene) chromophores present in the (b)Re–M dimers. Ruthenocene (Cp_2Ru) displays an absorption at $\bar{\nu}_{max} \approx 26\,000$ cm^{-1} and an emission at low temperature with $\bar{\nu}_{00} \approx 19\,000$ cm^{-1}; these transitions are assigned to absorption and emission from the lowest ^{3}d–d state ($^1A_{1g} \leftrightarrow a^3E_{1g}$).[57-59] Stern–Volmer studies of the rate at which Cp_2Ru quenches organic triplet excited-state donors suggests that ^{3}d–d lies at 22 000 cm^{-1}.[60] Ferrocene (Cp_2-Fe) displays an absorption at $\bar{\nu}_{max} \approx 19\,000$ cm^{-1}; however, no phosphorescence is observed from this compound even at low temperatures.[57] Stern–Volmer studies of the rate at which ferrocene quenches organic triplets suggests ^{3}d–d of this metallocene lies between 12 000 and 14 000 cm^{-1}.[60]

Because the ligand field strength of η^6-benzene may be less than that of η^5-cyclopentadienyl, the lowest ^{3}d–d state of CpM(arene) in the (b)Re–M dimers may lie at slightly lower energy compared to that for the respective Cp_2M complexes. In an effort gain direct spectroscopic information concerning the energy of ^{3}d–d in the CpRu(arene) unit, an emission spectrum of [CpRu(benzene)][PF$_6$] at 77 K in EtOH/MeOH (4:1 v/v) was recorded (Figure 4). This complex displays a broad, structureless emission with $\bar{\nu}_{max} \approx 19\,000$ cm^{-1} that can be assigned to luminescence from the lowest ^{3}d–d state. This result is consistent with the aforementioned studies on ruthenocene and indicates that the change from Cp_2Ru to CpRu(benzene) results in only a small decrease in the energy of the ^{3}d–d state. Taken together, all of the available data suggest that the energy of the lowest ^{3}d–d state in the CpM(arene) moieties in the (b)Re–M dimers is 12 000–14 000 cm^{-1} for M = Fe and 19 000–22 000 cm^{-1} for M = Ru.

Based on the above discussion of the energies of the Re → diimine MLCT state and the ^{3}d–d state of the CpM(arene) moieties, it is possible to provide qualitative estimates for ΔE_{E_NT} (Table 4). The values listed in Table 4 were calculated using $\bar{\nu}_{00}$ for the Re → diimine MLCT state (Table 1) and assuming $\bar{\nu}_{00}$(CpRu(arene)) = 20 500 and $\bar{\nu}_{00}$(CpFe(arene)) = 13 000 cm^{-1}. For the (b)Re–Ru series, it is probable that for all of the complexes $\Delta E_{E_NT} > 0$ and becomes less endothermic along the series bpy > dmb > tmb > deab. By contrast, intramolecular E_NT in (bpy)-Re–Fe is moderately exothermic.

Scheme 1 illustrates an excited-state diagram consistent with the observed photophysics and photochemistry of the (b)Re–Ru series. Photoexcitation into the MLCT absorption of the (b)-Re^{I}(CO)$_3$– chromophore leads to rapid production of the emissive ^{3}MLCT state. This excited state decays by normal radiative and nonradiative decay pathways (k_r and k_{nr}, respectively) in competition with endothermic E_NT (k_{E_NT}) to produce the ^{3}d–d state of CpRu(arene). Once formed, the ^{3}d–d state decays exceedingly rapidly, via either arene loss or nonradiative decay,[31,32] and consequently Re ^{3}MLCT → Ru ^{3}d–d E_NT is irreversible. The fraction of CpRu(arene) ^{3}d–d states that undergo permanent

(48) Hipps, K. W.; Crosby, G. A. *J. Am. Chem. Soc.* **1975**, *97*, 7042.
(49) Kober, E. M.; Meyer, T. J. *Inorg. Chem.* **1982**, *21*, 3967.
(50) Kober, E. M.; Meyer, T. J. *Inorg. Chem.* **1984**, *23*, 3877.
(51) Dexter, D. L. *J. Chem. Phys.* **1953**, *21*, 836.
(52) Förster, T. *Discuss. Faraday Soc.* **1959**, *27*, 7.
(53) Balzani, V.; Bolletta, V. *J. Am. Chem. Soc.* **1978**, *100*, 7404.
(54) Balzani, V.; Bolletta, G.; Scandola, F. *J. Am. Chem. Soc.* **1980**, *102*, 2152.
(55) Scandola, F.; Balzani, V. *J. Chem. Educ.* **1983**, *60*, 814.
(56) Saltiel, J.; Marchand, G.; Kirkor-Kaminska, E.; Smothers, W. K.; Mueller, W. B.; Charlton, J. L. *J. Am. Chem. Soc.* **1984**, *106*, 3144.
(57) Sohn, Y. S.; Hendrickson, D. N.; Gray, H. B. *J. Am. Chem. Soc.* **1971**, *93*, 3603.
(58) Crosby, G. A.; Hager, G. D.; Hipps, K. W.; Stone, M. L. *Chem. Phys. Lett.* **1974**, *28*, 497.
(59) Wrighton, M. S.; Pdungsap, L.; Morse, D. L. *J. Phys. Chem.* **1975**, *79*, 66.
(60) Chapple, A. P.; Vikesland, J. P.; Wilkinson, F. *Chem. Phys. Lett.* **1977**, *50*, 81.

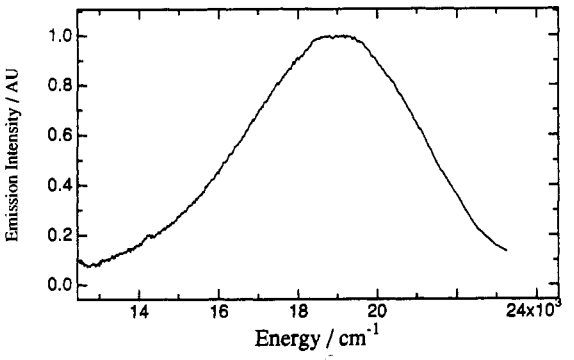

Figure 4. Corrected emission spectrum of [CpRu(benzene)][PF_6] in EtOH/MeOH (4:1 v/v) solvent glass at 77 K.

Table 3. Kinetic Parameters Obtained from Analysis of Temperature Dependence of Emission Decay[a]

complex	k_0/s^{-1}	k_1/s^{-1}	E_a^1/cm^{-1}	k_2/s^{-1}	E_a^2/cm^{-1}
(bpy)Re	3.7×10^6	1.9×10^7	610		
(dmb)Re	9.4×10^5	6.6×10^6	620		
(tmb)Re	5.9×10^5	4.0×10^6	490		
(deab)Re	4.1×10^4	8.4×10^6	760		
(bpy)Re–Ru	3.2×10^6	1.9×10^7	610	1.3×10^{10}	2330
(dmb)Re–Ru	7.9×10^5	6.6×10^6	620	1.5×10^{10}	2190
(tmb)Re–Ru	5.0×10^5	4.0×10^6	490	1.7×10^9	1670
(deab)Re–Ru	4.3×10^4	8.4×10^6	760	4.2×10^8	1230

[a] Emission decays in degassed butyronitrile/acetonitrile (70:30 v/v). See text for method of analysis.

Table 4. Energy-Transfer Rate Parameters for Re–Ru and Re–Fe Dimers[a]

complex	$\Delta E_{E_NT}/cm^{-1}$	k_{E_NT}/s^{-1}	k_2/s^{-1}	E_a^2/cm^{-1}	E_a^{calc}/cm^{-1} [d]
(bpy)Re–Ru	3000 ± 2000	3.6×10^4 [b]	1.3×10^{10}	2330	3000
(dmb)Re–Ru	2100 ± 2000	1.2×10^5 [b]	1.5×10^{10}	2190	2170
(tmb)Re–Ru	1400 ± 2000	5.3×10^5 [b]	1.7×10^9	1670	1670
(deab)Re–Ru	750 ± 2000	9.4×10^5 [b]	4.2×10^8	1230	1170
(bpy)Re–Fe	(−4500) ± 2000	3.4×10^8 [c]			

[a] Data calculated as described in text. [b] Estimated error ±50%. [c] Estimated error ±10%. [d] Activation energy calculated using the semiclassical expression with $\lambda = 3000\ cm^{-1}$.

photochemistry via arene loss is given by the parameter β. Direct irradiation of a series of CpRu(η^6-C_6H_5R) complexes (where C_6H_5R = alkyl-substituted benzenes) in CH_3CN solution indicates that arene loss occurs with quantum efficiency of ≈0.25.[24] Under the reasonable assumption that ^{3}d–d is formed with unit efficiency when CpRu(η^6-C_6H_5R) is directly excited, we take $\beta \approx 0.25$ in the (b)Re–Ru dimers.[24]

The excited-state diagram for (bpy)Re–Fe is analogous to that shown in Scheme 1, except that in this case E_NT is exothermic. The quantum efficiency for arene loss on direct irradiation of CpFe(η^6-C_6H_5R) complexes is ≈0.75, suggesting that for (bpy)-Re–Fe, $\beta \approx 0.75$.[24]

An important point is that because Re → Ru E_NT is endothermic in the (b)Re–Ru dimers, Ru → Re back E_NT is exothermic and is likely to be relatively rapid. Owing to this fact, it is important to justify the assumption that back E_NT is irreversible, because this assumption is used in the ensuing analysis of the experimental kinetic data. An excited-state kinetic model for the (b)Re–Ru dimers that includes back E_NT is given by eq 8. In this model, k_1 and k_2 are the rates of forward and back E_NT,

$$\text{(b)Re–Ru} \xleftarrow{k_4} {}^*\text{(b)Re–Ru} \underset{k_2}{\overset{k_1}{\rightleftarrows}} \text{(b)Re–}{}^*\text{Ru} \xrightarrow{k_3} \text{products} + \text{(b)Re–Ru} \quad (8)$$

respectively, k_3 is the decay rate of ^{3}d–d CpRu(arene), and k_4 is the decay rate of ^{3}MLCT (b)Re. A general expression is available in the literature that describes the temporal dependence of [*(b)Re–Ru] as a complex function of the rate constants k_1, k_2, k_3, and k_4.[61] This general expression was applied under the following constraints and assumptions that are appropriate for the (b)Re–Ru dimers: (1) $k_1/k_2 = \exp(-\Delta E_{E_NT}/RT)$; (2) $k_3 = 5 \times 10^{11}\ s^{-1}$;[31,32] (3) $k_1 < 10^7\ s^{-1}$. With these assumptions, it turns out that, for $1000\ cm^{-1} < \Delta E_{E_NT} < 2500\ cm^{-1}$, $k_2 \ll k_3$ and the observed first-order decay rate of *(b)Re–Ru is exactly equal to $k_1 + k_4$—in other words, Re → Ru E_NT is irreversible, as assumed in Scheme 1.

B. Rate Constants for E_NT in (b)Re–M Dimers. It is clear from the photophysical results that CpRu(arene) influences the nonradiative decay rate of the dimers in two opposing ways: (1) The "normal" nonradiative decay rate is *decreased* slightly in the dimers compared to the monomers. This effect is seen quite clearly by comparison of k_{nr} values for the bpy monomer–dimer pair at 298 K (Table 2). However, inspection of the temperature-dependent lifetime data reveals that at low temperatures the total decay rate (k_d) for the dmb and tmb dimers is *slower* than for the corresponding monomers. Since k_r is not strongly temperature dependent,[42] this observation indicates that the rate of "normal" nonradiative decay in these dimers is suppressed as well. One possible explanation for this effect is that the bulky CpRu(arene) unit partially shields (b)$Re^I(CO)_3$– from interacting with solvent, thereby slowing nonradiative decay via coupling of the MLCT state with librations of the polar solvent molecules.[46] (2) The total rate of nonradiative decay of the dimers is accelerated by Re → Ru E_NT. This effect is unambiguous from the 298 K emission data for the tmb and deab dimers: k_{nr} is significantly larger for the dimers compared to the corresponding monomers. However it is clear from the observation of photochemistry for the bpy and dmb dimers that E_NT occurs in these systems as well.

Since CpRu(arene) influences the "normal" nonradiative decay rate of the MLCT state (k_{nr}), it is not possible to determine the rate of E_NT (k_{E_NT}) from emission lifetimes of corresponding monomer–dimer pairs which is the "standard" technique for determining intramolecular rates of E_NT and ET in covalently linked chromophore–quencher compounds.[15] However, because E_NT leads to a permanent photochemical change, it is possible to estimate k_{E_NT} from a combination of emission lifetime and photochemical product quantum yield data. The rate for intramolecular Re → Ru E_NT can be calculated by using eq 11, which is derived by substituting the right side of eq 9 into eq 10 and rearranging. In these expressions Φ_{E_NT} is the quantum yield

$$\Phi_{E_NT} = \frac{k_{E_NT}}{k_r + k_{nr} + k_{E_NT}} = k_{E_NT}\tau_{dimer} \quad (9)$$

$$\Phi_P = \Phi_{E_NT}\beta \quad (10)$$

$$k_{E_NT} = \frac{\Phi_P}{\beta\tau_{dimer}} \quad (11)$$

for E_NT and the other parameters are defined above (see Scheme 1). Rate constants for E_NT in the (b)Re–Ru dimers, calculated by using the reaction quantum yields and the emission lifetime data in eq 11, are collected in Table 4. The calculated rate constants range from 3.6×10^4 to $9.4 \times 10^5\ s^{-1}$ and increase along the series bpy < dmb < tmb < deab, consistent with the fact that E_NT becomes less endothermic along the same series.

The emission quantum yield and lifetime of (bpy)Re–Fe are both decreased considerably compared to those of (bpy)Re, indicating that Re → Fe E_NT dominates overall decay of the MLCT excited state ($k_{E_NT} \gg k_r + k_{nr}$). In this case, k_{E_NT} can be calculated directly from the emission lifetime of the dimer

(61) Zimmerman, H. E.; Goldman, T. D.; Hirzel, T. K.; Schmidt, S. P. *J. Org. Chem.* **1980**, *45*, 3933.

Scheme 1

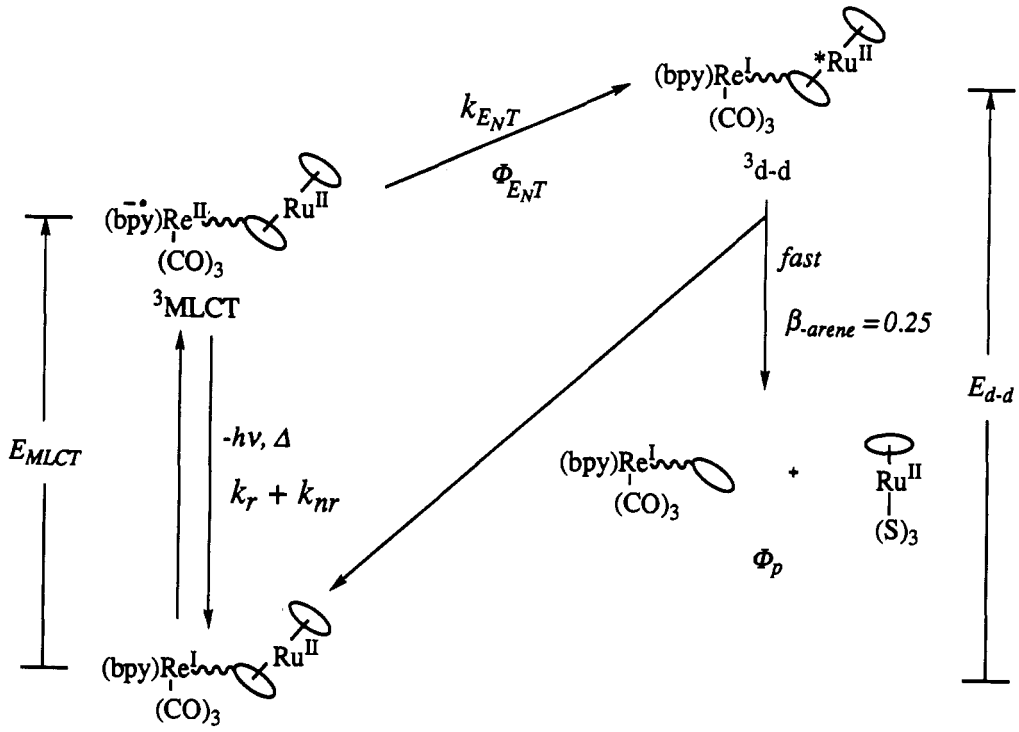

($k_{E_NT} = 1/\tau_{em}$(dimer); Table 4). Because $k_{E_NT} \gg (k_r + k_{nr})$ for (bpy)Re–Fe, the quantum efficiency for formation of the reactive ^{3}d–d state at CpFe(arene) is unity. In view of this fact, it is interesting that the observed quantum yield for arene loss in the dimer is 0.75, in very good agreement with the reported quantum yield for arene loss from CpFe(benzene) under direct irradiation (0.75).[24] This result substantiates the assumption that for CpFe(arene) the reactive ^{3}d–d state is formed with high efficiency under direct irradiation.

C. Temperature Dependence of Emission in (b)Re Monomers and (b)Re–Ru Dimers: Activation Parameters for E_NT. Because E_NT is endothermic in the Re–Ru dimers, the emission decay rate (k_d) for the dimers displays a strong temperature dependence (TD). If a significant component of the TD is due to activated Re → Ru E_NT, it should be possible to determine the activation energy and pre-exponential factor for E_NT.

A feature that complicates analysis of the dimer TD data is the fact that k_d for the (b)Re monomers varies weakly with temperature, indicating that the rate of "normal" nonradiative decay (k_{nr}) varies with temperature. In order to quantify this effect, the TD of k_d for the (b)Re monomers was fitted to eq 12

$$k_d(T) = k_0 + k_1 \exp\left(-\frac{E_a^1}{RT}\right) \qquad (12)$$

by nonlinear regression. This expression is based on a model in which k_d comprises a temperature-independent component, k_0, and a temperature-dependent component with frequency factor and activation energy, k_1 and E_a^1, respectively.[42,62,63] Table 3 contains the parameters obtained from regression analysis of the TD data for the four monomers, and the solid lines in Figure 3 were calculated using eq 12 and these parameters.

The TD of of the MLCT emission decay rate in other d^6 transition metal complexes is qualitatively similar to that observed for the (b)Re monomers when a ^{3}d–d state is not energetically accessible (via thermal activation) from the emissive MLCT state.[62] In these systems the temperature-dependent MLCT decay component is believed to arise from thermally activated nonradiative decay from a ^{3}MLCT state that is higher in energy than the lowest lying emissive ^{3}MLCT state.[62] Within this model, k_0 is the decay rate of the emissive MLCT state, k_1 is the decay rate from the thermally accessible state, and E_a^1 is the difference in energy between the two states. Consideration of the data in Table 3 within the context of this model suggests that for the (b)Re monomers there may be two ^{3}MLCT states that are separated by approximately 500 cm^{-1}, both having similar decay rates (10^5–10^7 s^{-1}).

Because k_{nr} is temperature dependent in the (b)Re monomers, it was expected that, in order to simulate the TD of k_d in the dimers, an expression containing two activated pathways would be required: one corresponding to the activated process observed in the monomers and another to thermally activated E_NT. Consistent with this expectation, analysis of the temperature dependence of k_d for the dimers reveals that the TD can only be fitted by using an expression of the form

$$k_d(T) = k_0 + k_1 \exp\left(-\frac{E_a^1}{RT}\right) + k_2 \exp\left(-\frac{E_a^2}{RT}\right) \qquad (13)$$

where k_0 is the rate of the temperature-independent decay component and k_i and E_a^i are the frequency factors and activation energies of the two activated pathways. In fitting the TD emission data for the (b)Re–Ru dimers, it was assumed that k_1 and E_a^1 are the same for the dimer and corresponding monomer.[64] The parameters obtained from regression analysis are provided in Table 3, and the solid lines that pass through the experimental data were calculated using these parameters in eq 13.

In the ensuing analysis of the dimer emission decay data, the temperature-independent and the first activated decay components (k_0, k_1, and E_a^1) are attributed to "normal" nonradiative decay of Re → diimine MLCT and the second activated decay component (k_2 and E_a^2) is attributed to Re → Ru E_NT. Several features are of interest with respect to the results listed in Table 3. First, for most of the dimer–monomer pairs, k_0 is smaller for

(62) Wacholtz, W. F.; Auerbach, R. A.; Schmehl, R. H. *Inorg. Chem.* **1986**, *25*, 227.
(63) Hager, G. D.; Crosby, G. A. *J. Am. Chem. Soc.* **1975**, *97*, 7031.
(64) In the regression analysis k_1 and E_a^1 for the dimers were fixed at the values obtained from the free-floating fits of the monomer temperature dependences.

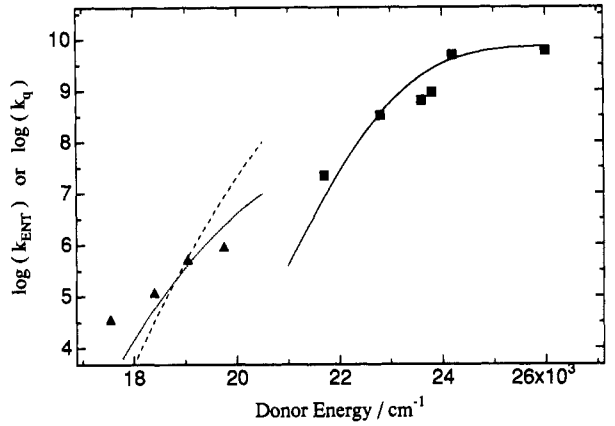

Figure 5. Plots of log(energy transfer rate) vs donor energy: (■) bimolecular E_NT from organic triplet donors to Cp_2Ru (data from ref 60); (▲) (b)Re–Ru dimers. Lines were calculated as described in the text.

the dimers. This is consistent with the point mentioned above that CpRu(arene) appears to decrease the rate of "normal" nonradiative decay in the dimers. Second, the frequency factor and activation energy of the second activated component (k_2 and E_a^2, respectively) vary systematically among the series of dimers: as $\bar{\nu}_{00}$ increases (ΔE_{E_NT} decreases), both k_2 and E_a^2 decrease.

The most significant finding of this experiment is the correlation between ΔE_{E_NT} and E_a^2, which is anticipated if the activated process corresponds to E_NT. Assuming that the calculated ΔE_{E_NT} values listed in Table 4 are correct and the E_a^2 values correspond to the activation energy for E_NT, by using the semiclassical expression (eq 6), the reorganization energy (λ) for E_NT is estimated to be 3000 cm^{-1}. Table 4 contains calculated values of the activation energy for E_NT obtained for each complex by using this value for λ. There is reasonably good correspondence between the observed E_a^2 values and the calculated values for all but one of the dimers. The calculated λ value is in accord with expectations based on the spectroscopic properties of the (b)-$Re^I(CO)_3$– chromophore[13,20] and the results of bimolecular quenching studies in which Cp_2Ru serves as a triplet energy acceptor (Figure 5; see below).[60]

An unexpected finding of the TD studies is the apparent decrease in the frequency factor (k_2) as ΔE_{E_NT} decreases.[65] As noted above, the frequency factor is proportional to the square of the donor/acceptor electronic coupling, V_{el}^2. Electronic coupling is expected to vary in proportion to the orbital overlap between the (b)$Re^I(CO)_3$– and CpRu(arene) chromophores. Since the members of the (b)Re–Ru series differ only in the nature of the substituents at the diimine ligand, V_{el} should remain comparatively constant across the series. Therefore, the frequency factor should remain constant for the series as well. Despite this anomaly, it is clear that k_2 is 3–4 orders of magnitude smaller than expected if E_NT is adiabatic (in this case, $k^\circ_{E_NT} \approx k_BT/h = 6 \times 10^{12}$ s^{-1}).[54] This suggests that although there is sufficient interaction between the Re and Ru chromophores to allow E_NT, the coupling is sufficiently weak that E_NT occurs only occasionally when the transition-state geometry is achieved (the process is significantly nonadiabatic).

D. Comparison of Intramolecular and Bimolecular E_NT Processes Involving the CpRu(arene) Chromophore. Wilkinson and co-workers examined the rate of bimolecular quenching of a series of organic triplet-excited-state donors by Cp_2Ru and demonstrated that the complex efficiently quenches donors with triplet energies greater than 21 000 cm^{-1}.[60] A plot comparing k_{E_NT} for the (b)Re–Ru series with the bimolecular quenching rate constants (k_q) obtained using Cp_2Ru as a triplet-state acceptor is provided in Figure 5. The donor energies used to construct this plot correspond to the energies of the organic triplet donors for the Cp_2Ru data set and to $\bar{\nu}_{00}$ values of the (b)$Re^I(CO)_3$–chromophores for the (b)Re–Ru complexes.

Both data sets were fit using the semiclassical expression (eq 6) to evaluate the dependence of k_{E_NT} on ΔE_{E_NT}. The bimolecular rate constants were evaluated using a rate expression of the form[54,56]

$$k_q = \frac{k_d}{1 + \exp\left(\frac{\Delta E_{E_NT}}{kT}\right) + \left(\frac{k_{-d}}{k_{E_NT}}\right)} \qquad (14)$$

where k_d and k_{-d} are rate constants for formation and dissociation of donor/acceptor encounter complexes and k_{E_NT} is the rate of E_NT within the encounter complex. The value of k_{E_NT} used in eq 14 was evaluated by using eq 6 with $\lambda = 3000$ cm^{-1} and $k^\circ_{E_NT} = 2.5 \times 10^{10}$ s^{-1}. The solid line that passes through the Cp_2Ru bimolecular quenching data in Figure 5 was calculated by assuming $\bar{\nu}_{00}(Cp_2Ru) = 23\,000$ cm^{-1}, $k_d = 1 \times 10^{10}$ M^{-1} s^{-1}, and $k_{-d} = 2 \times 10^{10}$ s^{-1}.[54,66] The rates for intramolecular E_NT in the (b)Re–Ru complexes were fit by using the unimolecular semiclassical rate expression directly. The dashed line in Figure 5 was calculated by assuming $\bar{\nu}_{00}$(CpRu(arene)) = 21 000 cm^{-1}, $k^\circ_{E_NT} = 2.5 \times 10^{10}$ s^{-1}, and $\lambda = 3000$ cm^{-1}, and the dotted line, with $\bar{\nu}_{00}$(CpRu(arene)) = 19 500 cm^{-1}, $k^\circ_{E_NT} = 5 \times 10^7$ s^{-1}, and $\lambda = 3000$ cm^{-1}. Note that the latter parameters provide a qualitatively better fit of the data for the (b)Re–Ru dimers.

Owing to the limited number of data points and relatively narrow ΔE_{E_NT} range spanned by both data sets, the parameters obtained from these fits should be viewed as tentative. However, in spite of this limitation, several conclusions can be drawn from the fits: (1) The two data sets cannot be fit using the same set of parameters, even taking into consideration the fact that one set involves a bimolecular reaction and the other is an intramolecular process. (2) The qualitative differences between the parameters required to fit the data imply that $\bar{\nu}_{00}$ for the CpRu-(arene) unit in the dimers is 2000–3000 cm^{-1} lower in energy compared to $\bar{\nu}_{00}$ for Cp_2Ru. (3) Assuming that λ is comparable in the two systems, the weaker dependence of k_{E_NT} on ΔE_{E_NT} in the dimers implies that $k^\circ_{E_NT}$ (electronic coupling) is 1–2 orders of magnitude smaller for intramolecular E_NT in the dimers than in the donor/acceptor encounter complexes in which E_NT occurs for the bimolecular system.

Conclusions

Photophysical and photochemical studies of the (b)Re–M dimers clearly establish that the Re → diimine MLCT chromophore transfers electronic excitation to the CpM(arene) unit, producing the reactive ^{3}d–d state of the latter chromophore. The rate and overall efficiency for intramolecular E_NT in the dimers increases substantially as the driving force for the process increases. Although the available kinetic data provide qualitative information concerning the reorganization energy and electronic coupling for Re → Ru E_NT, quantitative conclusions prove elusive because the absolute energies of the ^{3}MLCT and ^{3}d–d excited states of the donor and acceptor chromophores are not accurately known. Despite this limitation, the present investigation provides a paradigm for a unique approach to the study of endothermic intramolecular electronic energy-transfer processes.

Acknowledgment. We gratefully acknowledge support for this project from the National Science Foundation (Grant CHE-9123000).

(65) Significantly poorer fits result if k_2 is held constant across the series in the regression.

(66) Bock, C. R.; Connor, J. A.; Guitierrez, A. R.; Meyer, T. J.; Whitten, D. G.; Sullivan, B. P.; Nagle, J. K. *J. Am. Chem. Soc.* **1979**, *101*, 4815.